

Structural and decay properties of $Z = 132, 138$ superheavy nuclei

Asloob A. Rather¹, M. Ikram¹, A. A. Usmani¹, Bharat Kumar², S. K. Patra²

¹ Department of Physics, Aligarh Muslim University, Aligarh-202002, India.

² Institute of Physics, Bhubaneswar-751 005, India.

Received: date / Revised version: date

Abstract. In this paper, we analyze the structural properties of $Z = 132$ and $Z = 138$ superheavy nuclei within the ambit of axially deformed relativistic mean-field framework with NL3* parametrization and calculate the total binding energies, radii, quadrupole deformation parameter, separation energies, density distributions. We also investigate the phenomenon of shape coexistence by performing the calculations for prolate, oblate and spherical configurations. For clear presentation of nucleon distributions, the two-dimensional contour representation of individual nucleon density and total matter density has been made. Further, a competition between possible decay modes such as α -decay, β -decay and spontaneous fission of the isotopic chain of superheavy nuclei with $Z = 132$ within the range $312 \leq A \leq 392$ and $318 \leq A \leq 398$ for $Z = 138$ is systematically analyzed within self-consistent relativistic mean field model. From our analysis, we inferred that the α -decay and spontaneous fission are the principal modes of decay in majority of the isotopes of superheavy nuclei under investigation apart from β decay as dominant mode of decay in ^{318–322}138 isotopes.

PACS. PACS-key describing text of that key – PACS-key describing text of that key

1 Introduction

The quest for searching the limits on nuclear mass and charge in superheavy valley, which is still a largely unexplored area of research in nuclear physics, has been an intriguing endeavour for nuclear physics community from past several decades. In other words, the discovery of new elements with atomic number $Z > 102$ in the laboratory is being pursued with great vigour nowadays. The existence of superheavy nuclei (SHN) is the result of the interplay of the attractive nuclear force and the disruptive Coulomb repulsion between protons that favours fission. In principle, for SHN the shape of the classical nuclear droplet which is governed by surface tension and coulomb repulsion is unable to withstand the surface distortions making these nuclei susceptible to spontaneous fission. Thus, the stability of superheavy elements has become a long-standing fundamental nuclear science problem. Some of the topical issues that the nuclear physics community is looking to address in the superheavy regime of the nuclear chart are: how a nucleus with a large atomic number, such as $Z = 112$, survives the huge electrostatic repulsion between the protons, its physical and chemical properties, the extent of the superheavy region, i.e., to find an upper limit on the number of neutrons and protons that can be bound into one cluster, and the existence of very long-lived superheavy nuclei. Theoretically, the mere existence of the heaviest elements with $Z > 102$ is entirely due to quantal shell effects. However, in the midsixties, with

the invention of the shell-correction method, it was established that long-lived superheavy elements (SHE) with very large atomic numbers could exist due to the strong shell stabilization [1,2,3,4,5]. By incorporating shell effects, it shall be quite interesting to explore the regions in (Z, N) plane where long-lived superheavy nuclei might be expected. Exploration of (Z, N) plane in superheavy valley is driven by the understanding of not only the nuclear structure but also the structure of stars and the evolution of universe. Pursuing this line of thought, the pioneering work on superheavy elements was performed in 1960s [1,3,4,5] and such studies were quite successful in reproducing the already known half-lives by employing macroscopic-microscopic method (Nilsson-Strutinsky approach) with the folded-Yukawa deformed single-particle potential [6] and with the Woods-Saxon deformed single-particle potential [7,8,9]. Further, the outcome of these exhaustive investigations led to the understanding that the valley of superheavy nuclei is separated in proton and neutron number from known heavy elements by a region of much higher instability. In addition, several theoretical models which come under the aegis of macro-micro method like the fission model [10], cluster model [11], the density dependent M3Y(DDM3Y) effective model [12], the generalized liquid drop model (GLDM) [13] etc and self-consistent models like the relativistic mean field (RMF) theory [14], Skyrme Hartree-Fock (SHF) model [15] etc proved to be an effective tool for the successful description of α decay from heavy and SHN.

From the past three decades, the experimentalists have launched an expedition for predicting the ‘island of superheavy elements’, a region of increasing stable nuclei around $Z = 114$, which has led to a burst of activity in the superheavy regime. The synthesis of SHN in laboratory is accomplished by fusion of heavy nuclei above the barrier [16]. The two main processes employed for the synthesis of SHN are cold fusion performed mainly at GSI, Darmstadt and RIKEN Japan and hot fusion reactions performed at JINR-FLNR, Dubna. Until now, SHN with $Z \leq 118$ have been synthesized in the laboratory. The elements with $Z = 110, 111$ and 112 were produced in the experiments carried out at GSI [17,18,19,20,21]. The fusion cross section was extremely small in production of $Z = 112$ nucleus which led to the conclusion that the formation of further heavier elements would be very difficult by this process. The element with $Z = 113$ was identified at RIKEN, Japan [22,23] using cold fusion reaction with a very low cross section ~ 0.03 pb thus confirming the limitation of cold-fusion technique. The synthesis of $Z = 113 - 118$ was performed successfully by the experimentalists from joint collaboration of JINR-FLNR, Dubna and Lawrence Liverpool National Laboratory along with an unsuccessful attempt on the production of $Z = 120$ through hot fusion technique [24,25,26,27]. The isotopes of elements $Z = 112, 114, 116$ and 118 were identified in fusion-evaporation reactions at low excitation energies by irradiation of $^{233,238}\text{U}$, ^{242}Pu , ^{248}Cm and ^{248}Cf with ^{48}Ca beams [28]. The element $Z = 118$ and its immediate decay product, element with $Z = 116$, were produced at Berkeley Lab’s 88 inch cyclotron by bombarding targets of lead with an intense beam of high-energy krypton ions. The element ^{270}Hs with $Z = 108$ and $N = 162$ was synthesized by Dvorak et al. [29] by $^{26}\text{Mg} + ^{248}\text{Cm}$ reaction. Although the advancement in the accelerator facilities and the nuclear beam technologies have pushed the frontiers of nuclear chart especially in the superheavy region upto a great extent except for an attempt [30] to produce $Z = 120$ superheavy nuclei through the reaction $^{244}\text{Pu} + ^{58}\text{Fe}$, there has been until now no evidence for the production of nuclei with $Z > 118$. The short life times and the low production cross sections observed in fusion evaporation residues often increases the difficulty in synthesis of new superheavy nuclei and are posing a major difficulty to both theoreticians and experimentalists in understanding the various properties of superheavy nuclei.

Superheavy nuclei and their decay properties is one of the fastest growing fields in nuclear science nowadays. The discovery of alpha decay by Becquerel in 1896 and subsequently the alpha theory of decay proposed by Gamow, Condon and Gurnay in 1928 has ushered a new era in nuclear science. Quantum mechanically, α -decay occurs in heavy and superheavy nuclei by a tunnelling process through a coulomb barrier which is classically forbidden. The alpha decay [31,32,33,34,35,13] of the SHN is possible only if the shell effect supplies the extra binding energy and increases the barrier height of the fission. Thus, the beta stable nuclei with relatively longer half-life for spontaneous fission than that of alpha decay indicate that the

dominant decay mode for such a superheavy nucleus might be alpha decay. It is worth mentioning here that the α -decay is not the only mode of decay found in heavy nuclei but there is wealth of literature for β -decay, spontaneous fission (SF) and cluster decay also for such nuclei [36, 37,38,39,40,41,42,43,44]. Generally, alpha decay occurs in heavy and superheavy nuclei while as beta decay can occur throughout the periodic chart. The understanding of spontaneous fission and alpha decay on superheavy nuclei is rather more important than beta decay because the SHN with relative small alpha decay half-lives compared to SF half-lives will survive the fission and thus can be observed in the laboratory through alpha decay. Hence, the α -decay plays an indispensable role in the identification of new superheavy elements. Besides this, it has also been predicted that beta decay may play an important role for some of the superheavy nuclei [45]. However, β -decay proceeds through a weak interaction, the process is slow and less favoured compared to SF and alpha decay.

It is worth mentioning that the alpha decay and spontaneous fission are the main decay modes for both heavy and superheavy nuclei with $Z > 92$. Where, spontaneous fission acts as the limiting factor that decides the stability of superheavy nuclei and hence puts a limit on the number of chemical elements that can exist. It was Bohr and Wheeler [46] in 1939 who predicted and described the mechanism of spontaneous fission process on the basis of liquid drop model and established a limit of $\frac{Z^2}{A} \approx 48$, beyond which nuclei are unstable against spontaneous fission, and later in 1940, Flerov et. al. [47] observed this phenomenon in ^{235}U . This was followed by the several empirical formulas being proposed by various authors for calculating the half lives in spontaneous fission and the first attempt in this direction was made by Swiatecki [48] who proposed a semi-empirical formula for spontaneous fission. Further, Ren et. al. [49,50] proposed a phenomenological formula for calculating the spontaneous fission half-lives, and recently Xu et. al. [51] generalized an empirical formula for spontaneous fission half-lives of even-even nuclei. Here, in present manuscript, within the structural studies we made an attempt to look for the competition among various possible modes of decay such as α -decay, β -decay and SF of the isotopes of $Z = 132$ and $Z = 138$ superheavy elements with a neutron range $180 \leq N \leq 260$ and predict the possible modes of decay. The contents of the manuscript are organized as follows. The framework of relativistic mean-field formalism is outlined in section two. The results and discussion is presented in section three. Finally, section four contains the main summary and conclusions of this work.

2 Theoretical Formalism

From last few decades, the RMF theory has achieved a great success in describing many of the nuclear phenomena. Over the non-relativistic case, it is quite better to reproduce the structural properties of nuclei throughout the periodic table [52,53,54,55,56] near or far from the

stability lines including superheavy region [57]. The starting point of the RMF theory is the basic Lagrangian containing nucleons interacting with σ -, ω - and ρ -meson fields. The photon field A_μ is included to take care of the Coulomb interaction of protons. The relativistic mean field Lagrangian density is expressed as [52, 53, 54, 55, 56],

$$\begin{aligned}\mathcal{L} = & \bar{\psi}_i \{ i\gamma^\mu \partial_\mu - M \} \psi_i + \frac{1}{2} \partial^\mu \sigma \partial_\mu \sigma - \frac{1}{2} m_\sigma^2 \sigma^2 - \frac{1}{3} g_2 \sigma^3 \\ & - \frac{1}{4} g_3 \sigma^4 - g_s \bar{\psi}_i \psi_i \sigma - \frac{1}{4} \Omega^{\mu\nu} \Omega_{\mu\nu} + \frac{1}{2} m_\omega^2 V^\mu V_\mu \\ & - g_\omega \bar{\psi}_i \gamma^\mu \psi_i V_\mu - \frac{1}{4} B^{\mu\nu} B_{\mu\nu} + \frac{1}{2} m_\rho^2 R^\mu R_\mu - \frac{1}{4} F^{\mu\nu} F_{\mu\nu} \\ & - g_\rho \bar{\psi}_i \gamma^\mu \boldsymbol{\tau} \psi_i \mathbf{R}^\mu - e \bar{\psi}_i \gamma^\mu \frac{(1 - \tau_{3i})}{2} \psi_i A_\mu.\end{aligned}\quad (1)$$

Here M , m_σ , m_ω and m_ρ are the masses for nucleon, σ -, ω - and ρ -mesons and ψ is Dirac spinor. The field for the σ -meson is denoted by σ , ω -meson by V_μ and ρ -meson by R_μ . g_s , g_ω , g_ρ and $e^2/4\pi = 1/137$ are the coupling constants for the σ , ω , ρ -mesons and photon respectively. g_2 and g_3 are the self-interaction coupling constants for σ mesons. By using the classical variational principle, we obtain the field equations for the nucleons and mesons.

$$\begin{aligned}\{-\Delta + m_\sigma^2\} \sigma^0(r_\perp, z) = & -g_\sigma \rho_s(r_\perp, z) \\ & - g_2 \sigma^2(r_\perp, z) - g_3 \sigma^3(r_\perp, z),\end{aligned}\quad (2)$$

$$\{-\Delta + m_\omega^2\} V^0(r_\perp, z) = g_\omega \rho_v(r_\perp, z),\quad (3)$$

$$\{-\Delta + m_\rho^2\} R^0(r_\perp, z) = g_\rho \rho_3(r_\perp, z),\quad (4)$$

$$-\Delta A^0(r_\perp, z) = e \rho_c(r_\perp, z).\quad (5)$$

The Dirac equation for the nucleons is written by

$$\{-i\alpha \nabla + V(r_\perp, z) + \beta M^\dagger\} \psi_i = \epsilon_i \psi_i.\quad (6)$$

The effective mass of the nucleon is

$$M^\dagger = M + S(r_\perp, z) = M + g_\sigma \sigma(r_\perp, z),\quad (7)$$

and the vector potential is

$$V(r_\perp, z) = g_\omega V^0(r_\perp, z) + g_\rho \tau_3 R^0(r_\perp, z) + e \frac{(1 - \tau_3)}{2} A^0(r_\perp, z).\quad (8)$$

A static solution is obtained from the equations of motion to describe the ground state properties of nuclei. The set of nonlinear coupled equations are solved self-consistently in an axially deformed harmonic oscillator basis $N_F = N_B = 20$. The quadrupole deformation parameter β_2 is extracted from the calculated quadrupole moments of neutrons and protons through

$$Q = Q_n + Q_p = \sqrt{\frac{16\pi}{5}} \left(\frac{3}{4\pi} A R^2 \beta_2 \right),\quad (9)$$

where $R = 1.2A^{1/3}$.

The total energy of the system is given by

$$E_{total} = E_{part} + E_\sigma + E_\omega + E_\rho + E_c + E_{pair} + E_{c.m.},\quad (10)$$

where E_{part} is the sum of the single particle energies of the nucleons and E_σ , E_ω , E_ρ , E_c , E_{pair} , E_{cm} are the contributions of the meson fields, the Coulomb field, pairing energy and the center-of-mass energy, respectively. In present calculations, we use the constant gap BCS approximation to take care of pairing interaction [58]. We use non-linear NL3* parameter set [59] throughout the calculations.

3 Results and discussions

In this paper, we performed self-consistent relativistic mean field calculations by employing NL3* for calculating the binding energy, radii and quadrupole deformation β_2 for three different shape configurations. In Refs. [60, 61], $Z = 132, 138$ are suggested to be proton and $N = 198, 228, 238$ and 258 are neutron magic numbers. Therefore, we considered a range of neutron $N = 180 - 260$ that covers all these neutron magic numbers. These neutron as well as proton magic numbers form the doubly magic systems as $^{330}132$, $^{360}132$, $^{370}132$, $^{366}138$, $^{376}138$ and $^{396}138$. To analyze the structural properties of these isotopes, we made an attempt using deformed RMF calculations. It is well known that the superheavy nuclei are identified by α -decay in the laboratory followed by spontaneous fission. Therefore, to predict the possible mode of decay for the considered range of nuclides we make an investigation to analyze the competition between α -decay, β -decay and spontaneous fission which is considered to be central theme of the paper. The results are explained in subsections 3.1 to 3.6.

3.1 Selection of basis space

The RMF Lagrangian is used to obtain Dirac equation for Fermions and the Klein-Gordon equations for Bosons using state-of-the-art variational approach in a self-consistent manner. Further, these equations are solved in an axially deformed harmonic oscillator basis N_F and N_B for Fermionic and Bosonic wavefunction, respectively. For superheavy nuclei, a large number of basis space N_F and N_B is needed to get a convergent solution. For this, we have to choose an optimal model space for both Fermion and Boson fields. To choose optimal values for N_F and N_B , we select $^{312, 380}132$ systems as a test case and increase the basis number from 8 to 20 step by step. Results obtained for $^{312, 380}132$ systems using these basis space are shown in Fig 1. From our calculations, we notice an increment of 379 MeV in binding energy while going from $N_F = N_B = 8$ to 10 for $^{312}132$ system and it comes to be 48 MeV while N_F and N_B changes from 10 to 12 and further by increasing the number of basis a constant value of BE is obtained. Proceeding along the similar lines, for $^{380}132$ system, we notice a large increment in binding energy around 590 MeV when the basis change from 8 to 10 and this amount of BE reduces to 170 MeV while the basis (N_F and N_B) change from 10 to 12 and further a constant value of BE is obtained by increasing the basis space. This increment in energy decreases while going to higher oscillator basis. For example, change in binding energy is ≈ 0.2

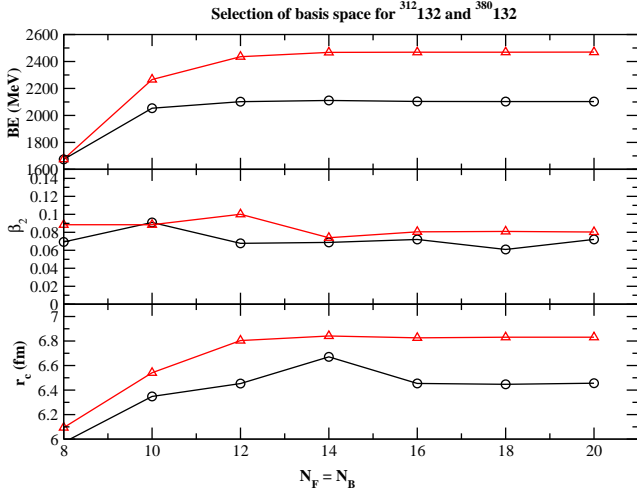


Fig. 1. (color online) The variation of calculated binding energy (BE), and quadrupole deformation parameter (β_2) and charge radius (r_c) are given with Bosonic and Fermionic basis. Black lines with circle represents the results for $^{312}_{132}$ and the outcome of $^{380}_{132}$ are shown by red line with triangle.

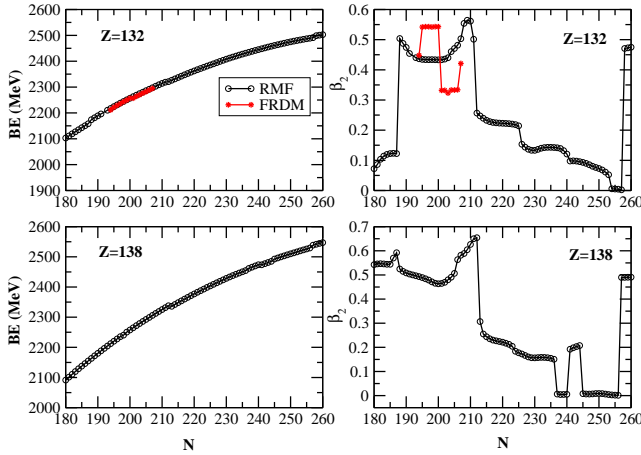


Fig. 2. (color online) Binding energy and deformation parameter as a function of neutron number.

and 0.6 MeV for $^{312}_{132}$ and $^{380}_{132}$ respectively with a change of $N_F = N_B$ from 18 to 20. Therefore, the present calculations dictate that the optimal basis sets to be chosen is $N_F = N_B = 20$ which is well within the convergence limits of the current RMF models.

3.2 Binding energy, radii and quadrupole deformation parameter

The calculated binding energy, radii and the quadrupole deformation parameter for the isotopic chains $^{312-392}_{132}$ and $^{318-398}_{138}$ are given in Tables 1 - 4 and plotted in Figures 2, 3. To find the ground state solution, the calculations are performed with an initial spherical, prolate and oblate quadrupole deformation parameter β_0 in the rela-

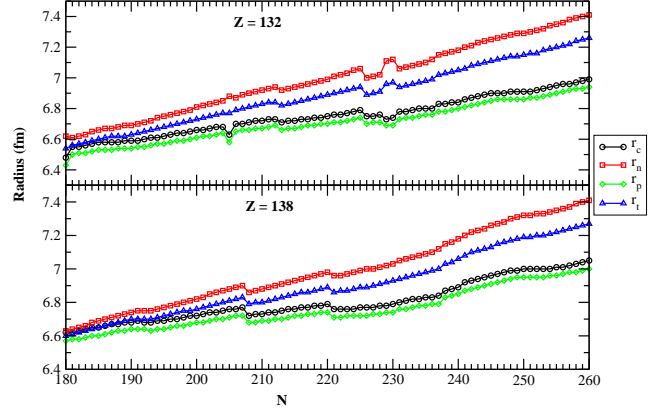


Fig. 3. (color online) Radii as a function of neutron number.

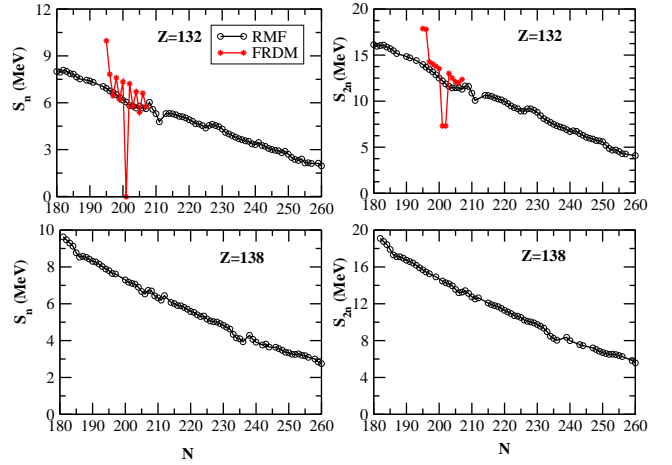


Fig. 4. (color online) One and two neutron separation energies as function of N

tivistic mean field formalism. It is important to mention here that maximum binding energy corresponds to the ground state energy and all other solutions are the intrinsic excited state configurations. Proceeding along these lines, we found prolate as a ground state for most of the cases. As the experimental binding energies for these superheavy isotopic chains are not available, in order to provide some validity to the predictive power of our calculations a comparison of binding energies of our calculations with those obtained from finite range droplet model (FRDM) [6] is made wherever available and close agreement is found. The calculated quadrupole deformation parameter from RMF and the values obtained from FRDM [6] predict the ground state of the considered isotopic chains to be prolate however there is a difference in magnitude as indicated in Table 1 as well as in Fig. 2. The radii monotonically increases with increasing number of neutrons. In general, the calculated binding energies are in good agreement with those of the FRDM values wherever available.

Table 1. Binding energy, deformation parameter and radii for Z=132 isotopic chain within three possible shape configurations.

Nuclei	BE			β_2			r_c			r_t			FRDM	
	sph.	prol.	obl.	sph.	prol.	obl.	sph.	prol.	obl.	sph.	prol.	obl.	BE	β_2
³¹² 132	2103.0		2159.2	0.073		-0.208	6.457		6.480	6.479		6.543		
³¹³ 132	2111.0		2118.0	0.086		-0.251	6.469		6.546	6.493		6.561		
³¹⁴ 132	2119.0		2126.0	0.102		-0.254	6.483		6.554	6.508		6.572		
³¹⁵ 132	2127.0		2133.8	0.112		-0.257	6.494		6.562	6.521		6.583		
³¹⁶ 132	2134.9		2141.4	0.118		-0.259	6.503		6.569	6.532		6.593		
³¹⁷ 132	2142.7		2148.9	0.121		-0.259	6.511		6.575	6.543		6.602		
³¹⁸ 132	2150.4		2156.2	0.122		-0.258	6.519		6.580	6.553		6.610		
³¹⁹ 132	2157.9		2163.5	0.121		-0.253	6.525		6.583	6.562		6.616		
³²⁰ 132	2165.2	2173.8	2170.8	0.118	0.496	-0.245	6.531	6.753	6.584	6.571	6.783	6.620		
³²¹ 132	2172.4	2181.3	2178.1	0.113	0.480	-0.237	6.535	6.744	6.585	6.578	6.778	6.624		
³²² 132	2179.6	2188.7	2185.4	0.104	0.467	-0.233	6.536	6.739	6.589	6.584	6.776	6.631		
³²³ 132	2186.6	2196.0	2192.6	0.091	0.447	-0.232	6.535	6.729	6.594	6.587	6.769	6.639		
³²⁴ 132	2193.7	2196.0	2199.7	0.080	0.447	-0.232	6.535	6.729	6.600	6.591	6.769	6.648		
³²⁵ 132	2200.7	2210.4	2206.7	0.072	0.433	-0.232	6.538	6.729	6.607	6.598	6.775	6.657		
³²⁶ 132	2207.7	2217.4	2213.6	0.067	0.429	-0.233	6.544	6.732	6.613	6.606	6.781	6.667	2211.5	0.448
³²⁷ 132	2214.6	2224.4	2220.3	0.061	0.425	-0.234	6.550	6.736	6.620	6.615	6.788	6.677	2221.5	0.542
³²⁸ 132	2221.3	2231.1	2226.9	0.057	0.420	-0.236	6.556	6.741	6.628	6.624	6.797	6.687	2229.3	0.543
³²⁹ 132	2227.8	2237.8	2233.4	0.050	0.421	-0.238	6.563	6.747	6.635	6.633	6.806	6.697	2235.8	0.543
³³⁰ 132	2234.3	2244.3	2239.7	0.000	0.428	-0.239	6.569	6.754	6.642	6.641	6.816	6.707	2243.4	0.542
³³¹ 132	2240.7	2250.7	2245.9	0.000	0.428	-0.241	6.577	6.761	6.649	6.651	6.826	6.718	2249.6	0.543
³³² 132	2246.7	2256.8	2252.1	0.000	0.426	-0.242	6.584	6.768	6.657	6.661	6.835	6.728	2256.9	0.543
³³³ 132	2252.5	2262.9	2258.2	0.007	0.427	-0.244	6.591	6.776	6.664	6.671	6.846	6.738	2256.9	0.332
³³⁴ 132	2258.4	2268.7	2264.2	0.031	0.429	-0.245	6.598	6.785	6.671	6.680	6.858	6.748	2264.1	0.332
³³⁵ 132	2264.4	2274.5	2270.1	0.051	0.434	-0.246	6.605	6.795	6.677	6.690	6.871	6.758	2269.9	0.323
³³⁶ 132		2280.1	2275.9		0.455	-0.248		6.817	6.684		6.896	6.767	2276.6	0.333
³³⁷ 132		2285.9	2294.1		0.469	-0.186		6.832	6.627		6.914	6.771	2281.9	0.333
³³⁸ 132		2291.6	2287.2		0.480	-0.251		6.780	6.697		6.933	6.787	2288.6	0.334
³³⁹ 132		2297.2	2292.7		0.494	-0.253		6.875	6.703		6.962	6.797	2294.3	0.421
³⁴⁰ 132		2303.2	2298.1		0.514	-0.255		6.933	6.710		7.021	6.807		
³⁴¹ 132		2308.8	2303.5		0.525	-0.257		6.949	6.716		7.040	6.817		
³⁴² 132		2314.1	2308.7		0.516	-0.259		6.950	6.722		7.045	6.827		
³⁴³ 132		2318.9	2314.0		0.456	-0.261		6.898	6.728		6.997	6.836		
³⁴⁴ 132		2321.0	2319.1		0.258	-0.260		6.707	6.733		6.819	6.844		
³⁴⁵ 132		2326.3	2324.0		0.248	-0.202		6.707	6.712		6.823	6.823		
³⁴⁶ 132		2331.6	2329.2		0.240	-0.201		6.709	6.717		6.828	6.831		
³⁴⁷ 132		2336.9	2334.4		0.233	-0.202		6.713	6.722		6.834	6.840		
³⁴⁸ 132		2342.2	2339.4		0.229	-0.203		6.717	6.727		6.841	6.849		
³⁴⁹ 132		2347.3	2344.3		0.226	-0.205		6.721	6.732		6.849	6.858		
³⁵⁰ 132		2352.4	2349.2		0.225	-0.207		6.726	6.738		6.857	6.867		
³⁵¹ 132		2357.4	2354.0		0.224	-0.209		6.731	6.743		6.866	6.876		
³⁵² 132		2362.3	2358.7		0.223	-0.212		6.735	6.749		6.874	6.886		
³⁵³ 132		2367.2	2363.4		0.222	-0.216		6.740	6.755		6.883	6.896		
³⁵⁴ 132		2371.8	2368.1		0.222	-0.221		6.745	6.761		6.892	6.906		
³⁵⁵ 132	2373.5	2376.5	2372.8	-0.01	0.219	-0.227	6.732	6.750	6.769	6.868	6.900	6.918		
³⁵⁶ 132		2381.0	2377.4		0.217	-0.237		6.755	6.780		6.909	6.932		
³⁵⁷ 132		2385.4	2382.0		0.214	-0.242		6.759	6.789		6.916	6.944		
³⁵⁸ 132		2389.9			0.155			6.748			6.906			
³⁵⁹ 132	2393.8	2394.5		0.001	0.145		6.752	6.752		6.901	6.913			
³⁶⁰ 132	2398.6	2399.1		0.001	0.138		6.758	6.757		6.910	6.921			
³⁶¹ 132	2403.0	2403.6	2387.6	0.001	0.135	-0.134	6.764	6.763	6.734	6.920	6.929	6.964		
³⁶² 132	2407.1	2407.9	2391.0	0.002	0.135	-0.139	6.770	6.768	6.739	6.929	6.938	6.974		
³⁶³ 132	2411.3	2412.0		0.005	0.136		6.777	6.773		6.939	6.948			
³⁶⁴ 132	2415.4	2416.0		0.014	0.140		6.783	6.777		6.949	6.957			
³⁶⁵ 132	2419.5	2419.9		0.023	0.142		6.790	6.782		6.959	6.966			
³⁶⁶ 132	2423.6	2423.7		0.024	0.143		6.796	6.786		6.969	6.976			
³⁶⁷ 132	2427.6	2427.4		0.013	0.143		6.803	6.791		6.979	6.985			

Table 2. Table I is continued.

Nuclei	BE			β_2			r_c			r_t		
	sph.	prol.	obl.	sph.	prol.	obl.	sph.	prol.	obl.	sph.	prol.	obl.
³⁶⁸ 132	2431.6	2431.1	2430.2	0.004	0.143	-0.083	6.81	6.796	6.803	6.989	6.994	6.988
³⁶⁹ 132	2435.5	2434.6	2433.4	0.002	0.142	-0.172	6.816	6.8	6.825	6.999	7.003	7.015
³⁷⁰ 132	2439.3	2438.2	2437.5	0.001	0.139	-0.176	6.822	6.804	6.831	7.008	7.011	7.026
³⁷¹ 132	2442.6	2441.5	2441.5	0.001	0.132	-0.179	6.825	6.806	6.837	7.017	7.017	7.036
³⁷² 132	2445.6	2444.8	2445.3	0.002	0.121	-0.183	6.828	6.806	6.843	7.025	7.022	7.046
³⁷³ 132	2448.5		2448.8	0.003		-0.197	6.83		6.855	7.033		7.061
³⁷⁴ 132	2451.4		2452.4	0.005		-0.214	6.831		6.870	7.041		7.077
³⁷⁵ 132	2454.3		2455.9	0.009		-0.223	6.833		6.881	7.049		7.091
³⁷⁶ 132	2457.2		2459.2	0.019		-0.229	6.834		6.891	7.056		7.104
³⁷⁷ 132	2460.8		2462.2	0.092		-0.230	6.821		6.897	7.058		7.114
³⁷⁸ 132	2463.8		2464.6	0.089		-0.228	6.824		6.902	7.066		7.122
³⁷⁹ 132	2466.7		2467.6	0.084		-0.224	6.827		6.904	7.074		7.129
³⁸⁰ 132	2469.6		2470.3	0.079		-0.218	6.831		6.906	7.083		7.135
³⁸¹ 132	2472.3		2473.1	0.076		-0.213	6.834		6.908	7.091		7.141
³⁸² 132	2475.1		2475.8	0.072		-0.209	6.837		6.910	7.099		7.148
³⁸³ 132	2477.6		2478.6	0.067		-0.205	6.839		6.913	7.107		7.155
³⁸⁴ 132	2479.9		2481.3	0.060		-0.205	6.841		6.918	7.115		7.164
³⁸⁵ 132	2482.3		2483.9	0.051		-0.208	6.842		6.926	7.123		7.175
³⁸⁶ 132	2484.7		2486.5	0.002		-0.213	6.853		6.936	7.137		7.187
³⁸⁷ 132	2486.9		2488.9	0.002		-0.219	6.853		6.946	7.144		7.199
³⁸⁸ 132	2488.9		2491.5	0.002		-0.224	6.852		6.955	7.151		7.212
³⁸⁹ 132	2491.2		2494.0	0.001		-0.228	6.851		6.964	7.158		7.223
³⁹⁰ 132	2493.2	2498.8	2496.4	0.001	0.471	-0.231	6.851	7.132	6.972	7.165	7.383	7.235
³⁹¹ 132	2495.2	2500.9	2498.5	0.000	0.473	-0.234	6.857	7.141	6.980	7.175	7.395	7.246
³⁹² 132	2496.8	2502.9	2500.4	0.007	0.475	-0.237	6.867	7.149	6.989	7.186	7.407	7.257
³⁹³ 132	2498.7	2504.8	2502.4	0.029	0.477	-0.240	6.879	7.158	6.998	7.197	7.419	7.269
³⁹⁴ 132	2500.8	2506.7	2504.3	0.046	0.479	-0.243	6.893	7.167	7.007	7.210	7.432	7.281
³⁹⁵ 132	2502.9	2508.7	2506.1	0.056	0.482	-0.247	6.907	7.176	7.016	7.222	7.444	7.293

3.3 Separation energy

The separation energy is an important observable in identifying the signature of magic numbers in nuclei. The magic numbers in nuclei are characterized by large shell gaps in their single-particle energy levels. This implies that the nucleons occupying the lower energy level have comparatively large value of energy than those nucleons occupying the higher energy levels, giving rise to more stability. The extra stability attributed to certain numbers can be predicted from the sudden fall in neutron separation energy. Two-neutron separation energy is more interesting which takes care of even-odd effects. The one and two-neutron separation energy is calculated by the difference in binding energies of two isotopes using the relations

$$\begin{aligned}
 S_n(N, Z) &= E_B(N, Z) - E_B(N - 1, Z) \\
 S_{2n}(N, Z) &= E_B(N, Z) - E_B(N - 2, Z)
 \end{aligned}
 \quad (11)$$

One- and two-neutron separation energy (S_n and S_{2n}) for the considered isotopic series of the nuclei ^{312–392}132 and ^{318–398}138 are shown in Figure 4. No sudden fall of the separation energies is observed for both the cases which indicates that as such no neutron magic behaviour within this force parameter is noticed.

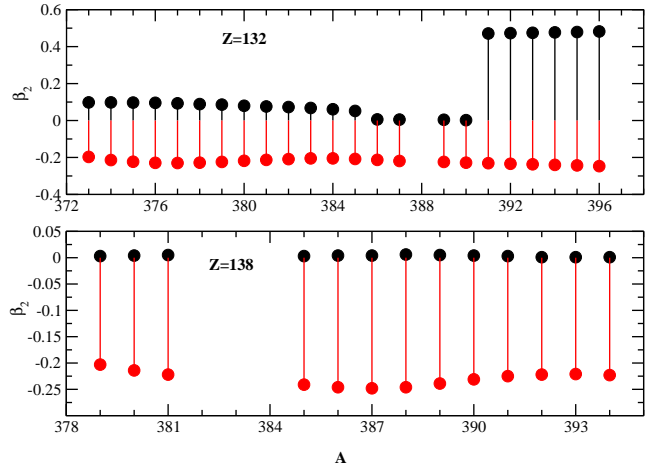


Fig. 5. (color online) Shape co-existence in $Z = 132$ and $Z = 138$ isotopic chain

3.4 Shape Coexistence

One of the remarkable properties of nuclear quantum many body systems is its ability to minimize its energy by assuming different shapes at the cost of relatively small energy compared to its total binding energy. Generally, the

Table 3. Same as Table 1 but Z=138 isotopic chain.

Nuclei	BE			β_2			r_c			r_t		
	sph.	prol.	obl.	sph.	prol.	obl.	sph.	prol.	obl.	sph.	prol.	obl.
³¹⁸ 138	2081.8	2091.4	2087.4	0.000	0.542	-0.260	6.508	6.809	6.615	6.506	6.788	6.600
³¹⁹ 138	2090.9	2101.0	2096.8	0.000	0.546	-0.263	6.513	6.817	6.623	6.513	6.799	6.611
³²⁰ 138	2099.7	2110.5	2106.0	0.000	0.547	-0.266	6.517	6.824	6.631	6.521	6.809	6.621
³²¹ 138	2108.5	2119.8	2114.9	0.000	0.546	-0.269	6.523	6.829	6.638	6.529	6.816	6.631
³²² 138	2117.1	2128.9	2123.7	0.001	0.544	-0.272	6.528	6.833	6.646	6.538	6.823	6.642
³²³ 138	2125.7	2137.7	2132.3	0.001	0.544	-0.275	6.534	6.838	6.653	6.547	6.831	6.652
³²⁴ 138	2134.2	2146.2	2140.7	0.002	0.570	-0.277	6.540	6.868	6.660	6.556	6.863	6.662
³²⁵ 138	2142.6	2154.8	2149.0	0.002	0.592	-0.279	6.547	6.896	6.667	6.565	6.892	6.672
³²⁶ 138	2151.1	2163.3	2157.2	0.003	0.525	-0.280	6.554	6.837	6.673	6.574	6.840	6.681
³²⁷ 138	2159.5	2171.7	2165.3	0.004	0.515	-0.280	6.561	6.834	6.679	6.584	6.840	6.690
³²⁸ 138	2167.9	2180.0	2173.2	0.005	0.508	-0.278	6.568	6.834	6.684	6.593	6.843	6.698
³²⁹ 138	2176.2	2188.3	2181.0	0.003	0.504	-0.272	6.575	6.836	6.686	6.602	6.848	6.702
³³⁰ 138	2184.5	2196.4	2188.9	0.002	0.500	-0.260	6.582	6.839	6.683	6.612	6.854	6.702
³³¹ 138	2192.9	2204.5	2196.8	0.001	0.497	-0.249	6.589	6.842	6.682	6.621	6.860	6.704
³³² 138	2201.1	2212.4	2204.7	0.001	0.493	-0.245	6.596	6.845	6.685	6.631	6.866	6.709
³³³ 138	2209.4	2220.2	2212.4	0.000	0.489	-0.243	6.603	6.848	6.690	6.640	6.871	6.717
³³⁴ 138	2217.6	2227.8	2220.1	0.000	0.484	-0.244	6.610	6.850	6.696	6.649	6.876	6.726
³³⁵ 138	2225.6	2235.4	2227.6	0.000	0.479	-0.244	6.616	6.851	6.703	6.658	6.881	6.735
³³⁶ 138	2233.3	2240.4	2235.0	0.000	0.471	-0.245	6.622	6.851	6.710	6.667	6.883	6.745
³³⁷ 138	2240.7	2250.3	2242.3	0.000	0.465	-0.247	6.628	6.853	6.716	6.676	6.887	6.754
³³⁸ 138	2247.7	2257.6	2249.5	0.000	0.463	-0.248	6.634	6.858	6.723	6.684	6.895	6.764
³³⁹ 138	2254.3	2264.8	2256.7	0.000	0.465	-0.248	6.639	6.867	6.730	6.693	6.907	6.773
³⁴⁰ 138	2261.1	2272.0	2263.7	0.000	0.470	-0.249	6.645	6.879	6.736	6.701	6.921	6.782
³⁴¹ 138	2267.6	2279.0	2270.7	0.001	0.480	-0.250	6.650	6.896	6.743	6.709	6.942	6.791
³⁴² 138	2274.0	2285.9	2277.0	0.001	0.491	-0.251	6.656	6.914	6.749	6.717	6.962	6.801
³⁴³ 138	2280.5	2292.5	2284.1	0.003	0.506	-0.252	6.661	6.936	6.756	6.726	6.986	6.810
³⁴⁴ 138	2287.0	2299.1	2290.6	0.010	0.563	-0.254	6.667	6.995	6.762	6.734	7.046	6.820
³⁴⁵ 138	2293.4	2305.8	2297.0	0.025	0.582	-0.256	6.674	7.020	6.769	6.743	7.072	6.829
³⁴⁶ 138	2300.0	2312.5	2301.8	0.038	0.589	-0.158	6.681	7.033	6.722	6.753	7.089	6.787
³⁴⁷ 138	2306.4	2319.0	2308.4	0.050	0.604	-0.157	6.690	7.054	6.728	6.763	7.112	6.795
³⁴⁸ 138	2312.9	2325.2	2314.8	0.095	0.627	-0.157	6.706	7.078	6.733	6.780	7.139	6.803
³⁴⁹ 138		2331.4	2321.0		0.650	-0.157		7.103	6.739		7.166	6.812
³⁵⁰ 138		2337.9	2327.1		0.654	-0.157		7.113	6.744		7.180	6.820
³⁵¹ 138		2336.0	2333.2		0.307	-0.158		6.800	6.750		6.879	6.829
³⁵² 138		2342.1	2339.0		0.255	-0.159		6.771	6.756		6.857	6.838
³⁵³ 138		2348.1	2344.9		0.244	-0.161		6.772	6.762		6.860	6.847
³⁵⁴ 138		2354.0	2350.7		0.235	-0.162		6.774	6.768		6.865	6.856
³⁵⁵ 138		2359.9	2356.4		0.230	-0.163		6.778	6.774		6.872	6.864
³⁵⁶ 138		2365.7	2361.9		0.227	-0.163		6.782	6.779		6.879	6.873
³⁵⁷ 138		2371.4	2367.4		0.224	-0.163		6.787	6.783		6.887	6.881
³⁵⁸ 138		2377.0	2372.9		0.221	-0.161		6.791	6.787		6.894	6.888
³⁵⁹ 138		2382.5	2380.0		0.217	-0.158		6.795	6.757		6.902	6.862
³⁶⁰ 138		2387.9	2385.8		0.212	-0.151		6.800	6.760		6.909	6.868
³⁶¹ 138	2391.5	2393.2		0.019	0.204		6.758	6.803		6.871	6.915	
³⁶² 138	2397.2	2398.6		0.005	0.183		6.761	6.804		6.877	6.918	
³⁶³ 138	2403.0	2403.7		0.003	0.178		6.765	6.809		6.885	6.924	
³⁶⁴ 138	2408.8	2408.8		0.002	0.173		6.770	6.813		6.892	6.932	
³⁶⁵ 138	2414.4	2413.8		0.001	0.166		6.774	6.816		6.900	6.938	
³⁶⁶ 138	2419.7	2418.8		0.001	0.160		6.779	6.820		6.908	6.945	
³⁶⁷ 138	2424.8	2423.8		0.001	0.157		6.784	6.825		6.917	6.953	
³⁶⁸ 138	2429.6	2428.6		0.002	0.156		6.790	6.830		6.926	6.961	
³⁶⁹ 138	2434.2	2433.3		0.003	0.157		6.795	6.835		6.935	6.970	
³⁷⁰ 138	2438.8	2437.9		0.005	0.158		6.801	6.839		6.944	6.978	
³⁷¹ 138	2443.5	2442.3		0.008	0.158		6.807	6.844		6.954	6.987	
³⁷² 138	2448.0	2446.4		0.009	0.157		6.813	6.848		6.963	6.995	
³⁷³ 138	2452.6	2450.5		0.006	0.155		6.818	6.852		6.972	7.003	

Table 4. Table III is continued.

Nuclei	BE			β_2			r_c			r_t		
	sph.	prol.	obl.	sph.	prol.	obl.	sph.	prol.	obl.	sph.	prol.	obl.
³⁷⁴ 138	2457.1	2454.5		0.004	0.151		6.824	6.855		6.981	7.010	
³⁷⁵ 138	2461.6			0.002			6.829			6.989		
³⁷⁶ 138	2465.9		2465.7	0.002		-0.150	6.833		6.874	6.998		7.032
³⁷⁷ 138	2469.9		2470.2	0.002		-0.159	6.837		6.883	7.006		7.044
³⁷⁸ 138	2473.9		2474.7	0.002		-0.167	6.839		6.892	7.014		7.056
³⁷⁹ 138	2477.7	2473.7	2478.9	0.003	0.192	-0.203	6.841	6.908	6.918	7.021	7.075	7.083
³⁸⁰ 138	2481.5	2477.5	2483.3	0.004	0.198	-0.214	6.843	6.919	6.930	7.028	7.087	7.097
³⁸¹ 138	2485.3	2481.3	2487.7	0.005	0.203	-0.222	6.845	6.929	6.940	7.036	7.100	7.110
³⁸² 138	2488.9	2484.9	2491.8	0.005	0.207	-0.226	6.847	6.938	6.949	7.043	7.111	7.122
³⁸³ 138	2492.6		2495.5	0.003		-0.229	6.849		6.957	7.051		7.133
³⁸⁴ 138	2496.3		2499.0	0.003		-0.235	6.852		6.965	7.058		7.145
³⁸⁵ 138	2499.8		2502.5	0.003		-0.241	6.854		6.975	7.066		7.157
³⁸⁶ 138	2503.3		2505.9	0.004		-0.246	6.857		6.985	7.075		7.169
³⁸⁷ 138	2506.7		2509.2	0.004		-0.248	6.860		6.992	7.083		7.180
³⁸⁸ 138	2509.9		2512.4	0.006		-0.246	6.863		6.996	7.091		7.187
³⁸⁹ 138	2513.4		2515.5	0.005		-0.239	6.866		6.997	7.100		7.192
³⁹⁰ 138	2516.6		2518.8	0.004		-0.231	6.868		6.998	7.108		7.196
³⁹¹ 138	2519.9		2521.9	0.003		-0.225	6.871		6.999	7.117		7.201
³⁹² 138	2523.0		2525.3	0.001		-0.222	6.873		7.002	7.125		7.208
³⁹³ 138	2526.3		2528.6	0.001		-0.221	6.876		7.007	7.134		7.216
³⁹⁴ 138	2529.4		2531.8	0.001		-0.223	6.879		7.014	7.142		7.226
³⁹⁵ 138	2532.4	2538.7	2534.9	0.000	0.489	-0.226	6.882	7.194	7.021	7.151	7.399	7.236
³⁹⁶ 138	2535.3	2541.7	2537.8	0.000	0.490	-0.229	6.887	7.201	7.029	7.160	7.409	7.247
³⁹⁷ 138	2537.9	2544.6	2540.7	0.000	0.490	-0.232	6.893	7.207	7.037	7.170	7.419	7.258
³⁹⁸ 138	2540.4	2547.3	2543.5	0.000	0.491	-0.235	6.901	7.214	7.045	7.180	7.429	7.269
³⁹⁹ 138	2542.7	2550.2	2546.2	0.001	0.491	-0.238	6.910	7.222	7.054	7.190	7.439	7.281
⁴⁰⁰ 138	2545.1	2553.1	2548.8	0.001	0.492	-0.241	6.919	7.229	7.063	7.200	7.450	7.292
⁴⁰¹ 138	2547.4	2555.9	2551.4	0.003	0.494	-0.245	6.928	7.236	7.072	7.210	7.461	7.303

nuclei having different binding energies correspond to their different shape configurations leads to the ground as well as intrinsic excited states. However, in certain cases it may happen that the binding energy of two different shape configurations may coincide or very close to each other and this phenomenon is known as shape coexistence [62, 63, 64]. This phenomenon is more common in superheavy region giving rise to complex structures in these nuclei and thus enriching our understanding of the oscillations occurring between two or three existing shapes. In the isotopic chains discussed here in the paper, we have come across many examples where the ground and first excited binding energies are degenerate. In the isotopic chain of ^{180–260}132, we noticed the co-existence of shape (oblate-prolate, oblate-spherical) for ^{373–387}132 and ^{389–396}132 isotopes as shown in Fig. 5. In present analysis, we consider a binding energy difference less or equal to 2 MeV for marking the shape co-existence. Due to this small binding energy difference the ground-state can change to low-lying excited state or vice versa by making a small change in the input parameters like the pairing energy. The shape co-existence in nuclei indicates the competition between the different shape configurations differing from each other by a small amount in binding energy so as to acquire the ground state energy with maximum stability and the final shape could be a superposition of these low-lying bands. Further, in the isotopic chain of ^{180–260}138, we noticed

the shape co-existence (oblate-spherical) for ^{379–381}138 and ^{385–394}138 as shown in Fig. 5. Thus present analysis reveals that some of the nuclei of considered isotopic chain oscillate oblate-spherical as well as oblate-prolate and vice-versa.

3.5 Density distribution

Density distribution provides a detailed information regarding the distribution of nucleons for identifying central depletion in density, long tails and clusters in density plots. These features are known by bubble, halo and cluster structures of the nuclei and may be observed in light to superheavy nuclei [65, 66, 67, 68, 69, 70]. Here, we have plotted the density profile for neutron, proton and total matter (neutron plus proton) for some of the predicted closed shell nuclei [60, 61] within this framework as shown in Figs. 6, 7. Some of the nuclei for example; ³⁶⁰132 and ³⁷⁰132 show the depletion of central density on ground state as well as intrinsic excited states. The strength of bubble shape is evaluated by calculating the depletion fraction [68, 69]. There is no depletion of central density as such for ³⁶⁶138, ³⁷⁶138, ³⁹⁶138 systems. Some nuclei such as ³⁶⁰132 and ³⁷⁰132 indicate a special kind of nucleon distribution. In these cases, the centre is slightly bulgy and a considerably depletion afterward but again a

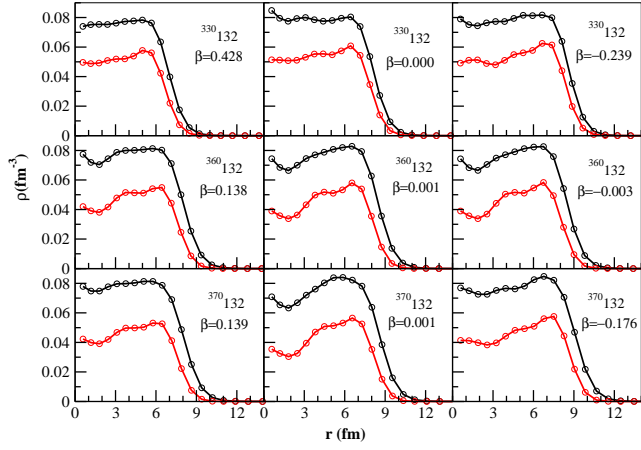


Fig. 6. (color online) Density profile for some selected nuclei on ground as well as intrinsic excited states. The black line with circle represents the neutron density and proton density is shown by red line with red circle.

big hump at mid of the centre and the surface. To reveal such type of distribution and to gain an insight into the arrangement of nucleons, we make two-dimensional contour plots for $^{360}_{132}$ and $^{370}_{132}$ with three different shape configurations as given in Figs. 8 and 9. Figures 6 and 8 reflect that the hollow region at the centre is spread over the radius of 1 – 3 fm. This may suggest that these nuclei might have fullerene type structure and cluster of neutron and alpha-particle might be possibly within these types of nuclei. The full black contour refers to maximum density and full white ones to zero density region. It is apparent from figure 8 that the central portion of total matter density distribution in $^{360}_{132}$ within spherical configuration is less dense than the peripheral region which can be interpreted as a thin gas of nucleons being surrounded by a thick sheath of nucleon (high density) giving rise to a bubble-type structure. The individual neutron and proton density distributions also support the same bubble like structure within this shape configuration. We witnessed a cluster type structure in total matter density distribution for oblate, spherical and prolate shape configurations. For the case of $^{370}_{132}$ (Fig 9), the two dimensional contour representation reveals that the total proton density distribution assumes a cluster shape for oblate and prolate configurations with $\beta_2 = -0.25, 0.14$ respectively. Whereas in case of spherical and prolate cases, the proton and total matter density distribution appears to be as bubble type, respectively. We noticed a semi-bubble like structure for the total nucleonic density distribution within the spherical case. The neutron density distribution plot for the oblate shape configuration appears to be spindle shaped with prominent flaps/bulges. Further, inspection reveals that the central part ($r = 0$ fm) is considerably populated in proton density distribution but the depopulation is noticed at $r = 1$ to $r = 3$ fm and further a large population in proton density distribution beyond 3 fm is evident that goes to zero at the surface.

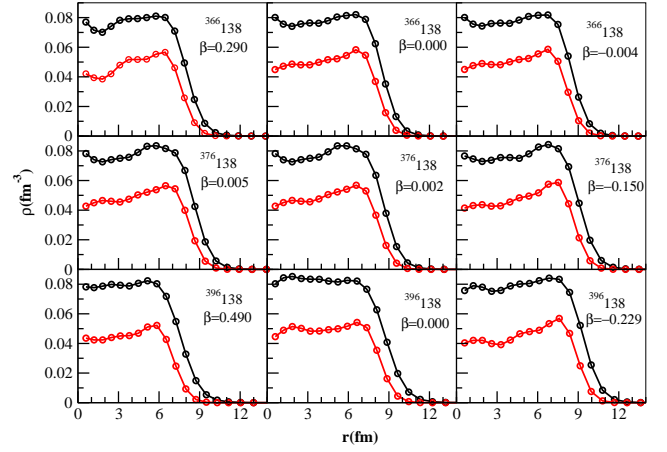


Fig. 7. (color online) Same as Fig. 6 but for $^{366,376,396}_{138}$.

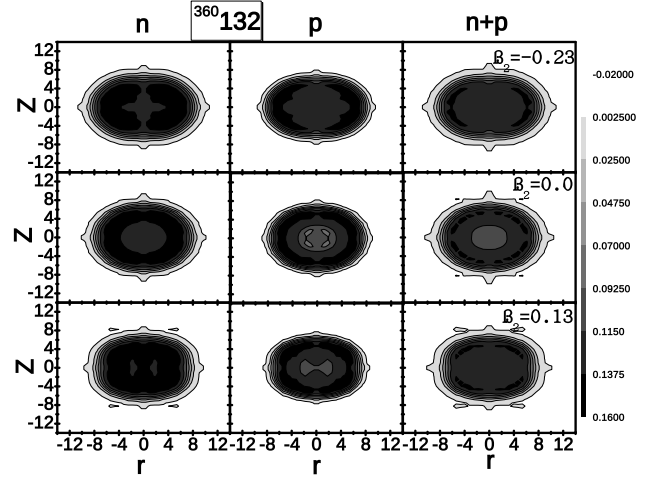


Fig. 8. Two dimensional neutron, proton and neutron plus proton density contours of $^{360}_{132}$ nucleus for three different shape configurations.

3.6 Decay-energy and half-life

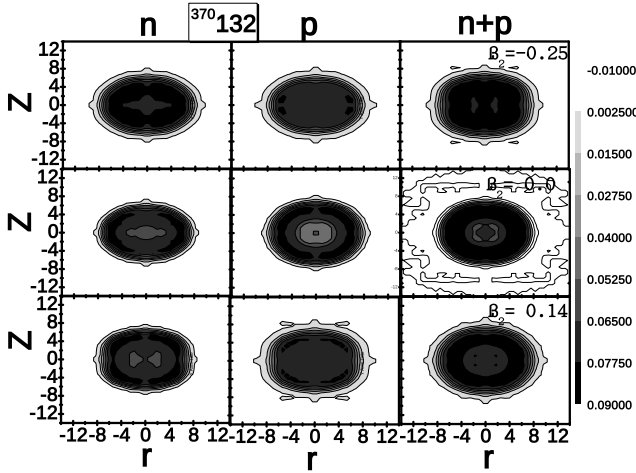
In order to predict the modes of decay of the considered nuclides, the α -decay, β -decay and SF half-lives shall be computed using various empirical formulas and their comparison of life-time shall predict the dominant mode of decay. To analyze the dominant mode of decay(alpha), the alpha decay half-lives are estimated using various empirical formulas such as Viola-Seaborg (VSS) [71], generalized liquid drop model (GLDM) [72], Brown [73], Royer [74], NI et al. [75]. Spontaneous fission half-lives are computed using the semi-empirical formula of Ren and Xu [76] and made a comparison with alpha decay half lives to predict a possible decay mode of considered nuclides. The beta decay half-lives are estimated using empirical formulas of Fiset and Nix [77].

Table 5. Decay energies and half-lives of α , β and spontaneous fission for $Z = 132$ isotopic chains.

Nuclei	Q_{α}^{RMF}	Q_{α}^{FRDM}	$\log(T_{1/2}^{\alpha})$						$\log(T_{SF})$	Q_{β}^{RMF}	Q_{β}^{FRDM}	Fiset-Nix		FRDM	Mode of
	MeV	MeV	FRDM	VSS	GLDM	Brown	Royer	Ni et. al.	Ren-Xu	MeV	MeV	$\log(T_{1/2}^{\beta})$	$T_{1/2}^{\beta}(\text{sec})$	$T_{1/2}^{\beta}(\text{sec})$	decay
³¹² 132	17.70			-10.49	-10.33	-9.30	-9.70	-10.82	97.40	11.07		-0.08	0.84		α
³¹³ 132	17.50			-9.14	-9.15	-9.06	-9.44	-9.83	83.03	10.86		-0.53	0.30		α
³¹⁴ 132	17.14			-9.68	-9.56	-8.62	-8.93	-10.13	103.83	10.82		-0.02	0.96		α
³¹⁵ 132	16.82			-8.13	-8.19	-8.22	-8.47	-8.97	87.03	10.74		-0.50	0.32		α
³¹⁶ 132	16.68			-8.98	-8.91	-8.04	-8.28	-9.53	105.63	10.5		0.06	1.15		α
³¹⁷ 132	16.51			-7.65	-7.74	-7.81	-8.03	-8.56	86.67	10.21		-0.37	0.43		α
³¹⁸ 132	16.48			-8.67	-8.63	-7.78	-8.00	-9.27	102.89	9.89		0.21	1.63		α
³¹⁹ 132	16.39			-7.46	-7.59	-7.66	-7.88	-8.40	82.01	9.56		-0.20	0.63		α
³²⁰ 132	16.34			-8.45	-8.45	-7.59	-7.82	-9.08	95.68	8.58		0.57	3.68		α
³²¹ 132	16.30			-7.32	-7.48	-7.54	-7.77	-8.28	73.13	8.42		0.12	1.30		α
³²² 132	16.05			-7.98	-8.02	-7.19	-7.39	-8.68	84.09	8.17		0.69	4.89		α
³²³ 132	15.92			-6.70	-6.90	-7.01	-7.19	-7.75	60.13	8.08		0.22	1.66		α
³²⁴ 132	14.38			-5.01	-5.10	-4.70	-4.48	-6.14	68.20	7.95		0.76	5.74		α
³²⁵ 132	14.28			-3.75	-4.00	-4.54	-4.30	-5.23	43.07	7.63		0.36	2.30		α
³²⁶ 132	14.19	16.01	-7.92	-4.64	-4.77	-4.39	-4.14	-5.82	48.10	7.36	8.70	0.95	8.92	0.29	α
³²⁷ 132	13.99	12.04	1.22	-3.17	-3.47	-4.05	-3.76	-4.74	22.03	7.07	6.28	0.55	3.56	0.81	α
³²⁸ 132	13.95	11.57	1.38	-4.16	-4.33	-3.99	-3.70	-5.41	23.85	6.76	4.88	1.16	14.45	1.48	α
³²⁹ 132	13.84	14.05	-3.30	-2.87	-3.20	-3.80	-3.50	-4.48	-2.92	6.43	5.73	0.78	6.08	1.81	α
³³⁰ 132	13.75	13.99	-4.23	-3.75	-3.96	-3.64	-3.33	-5.06	-4.46	6.07	4.30	1.42	26.47	2.34	SF
³³¹ 132	13.69	13.99	-3.02	-2.56	-2.92	-3.54	-3.22	-4.21	-31.71	5.70	5.16	1.08	11.93	1.81	SF
³³² 132	13.61	13.85	-3.96	-3.46	-3.71	-3.40	-3.07	-4.82	-36.76	5.34	3.61	1.73	53.97	4.28	SF
³³³ 132	13.53	19.75	-12.10	-2.22	-2.62	-3.26	-2.92	-3.92	-64.27	4.98	10.32	1.40	25.16	0.41	SF
³³⁴ 132	13.49	19.54	12.92	-3.20	-3.49	-3.19	-2.86	-4.60	-72.99	4.65	3.45	2.06	15.38	8.71	SF
³³⁵ 132	13.38	13.88	-2.94	-1.90	-2.34	-2.99	-2.64	-3.65	-100.53	4.35	4.12	1.72	52.64	15.82	SF
³³⁶ 132	13.36	19.20	-12.50	-2.93	-3.25	-2.95	-2.61	-4.36	-113.06	4.14	2.83	2.34	16.89	15.69	SF
³³⁷ 132	13.14	14.40	-3.45	-1.38	-1.85	-2.55	-2.15	-3.20	-140.42	4.01	4.19	1.91	81.90	11.55	SF
³³⁸ 132	12.90	14.04	-4.34	-1.91	-2.27	-2.10	-1.64	-3.49	-156.92	3.91	2.70	2.47	96.07	18.05	SF
³³⁹ 132	12.72	13.33	-1.80	-0.43	-0.94	-1.75	-1.24	-2.39	-183.89	3.71	3.07	2.10	24.50	>100	SF
³⁴⁰ 132	11.98			0.31	-0.11	-0.24	0.52	-1.60	-204.50	3.66		2.63	22.74		SF
³⁴¹ 132	11.76			1.94	1.38	0.24	1.07	-0.37	-230.87	3.16		2.46	89.71		SF
³⁴² 132	11.78			0.82	0.37	0.19	1.00	-1.16	-255.72	2.77		3.25	96.69		SF
³⁴³ 132	12.13			0.99	0.41	-0.56	0.10	-1.18	-281.29	1.99		3.47	17.53		SF
³⁴⁴ 132	12.86			-1.82	-2.28	-2.02	-1.64	-3.41	-310.54	2.75		3.27	76.72		SF
³⁴⁵ 132	12.29			0.60	-0.02	-0.89	-0.32	-1.52	-335.10	3.12		2.50	13.69		SF
³⁴⁶ 132	12.26			-0.39	-0.90	-0.83	-0.27	-2.20	-368.87	2.90		3.16	42.81		SF
³⁴⁷ 132	12.06			1.17	0.52	-0.41	0.21	-1.03	-392.24	2.73		2.80	24.58		SF
³⁴⁸ 132	11.85			0.64	0.09	0.04	0.72	-1.32	-430.67	2.55		3.44	81.75		SF
³⁴⁹ 132	11.64			2.25	1.56	0.50	1.25	-0.10	-452.65	2.35		3.12	29.10		SF
³⁵⁰ 132	11.55			1.43	0.84	0.70	1.47	-0.64	-495.88	2.17		3.79	4.75		SF
³⁵¹ 132	11.49			2.66	1.93	0.84	1.62	0.24	-516.28	2.01		3.46	59.16		SF
³⁵² 132	11.50			1.56	0.94	0.82	1.58	-0.53	-564.43	1.82		4.16	63.51		SF
³⁵³ 132	11.52			2.58	1.82	0.77	0.21	0.17	-583.06	1.62		3.90	92.65		SF
³⁵⁴ 132	11.66			1.14	0.48	0.46	1.12	-0.89	-636.28	1.42		4.65	74.39		SF
³⁵⁵ 132	11.70			2.10	1.31	0.37	1.00	-0.24	-652.96	1.25		4.40	65.44		SF
³⁵⁶ 132	11.71			1.00	0.31	0.35	0.96	-1.01	-711.35	-1.05		5.21	74.66		SF
³⁵⁷ 132	11.81			1.81	0.99	0.13	0.68	-0.48	-725.91	0.83		5.11	38.01		SF
³⁵⁸ 132	11.58			1.35	0.62	0.64	1.27	-0.71	-789.61	0.89		5.50	49.32		SF
³⁵⁹ 132	11.21			3.43	2.57	1.49	2.26	0.90	-801.86	0.73		5.32	47.56		SF
³⁶⁰ 132	10.83			3.46	2.69	2.41	3.33	1.09	-870.99	0.57		6.18	96.70		SF
³⁶¹ 132	10.45			5.68	4.77	3.38	4.46	2.82	-880.77	0.38		6.20	12.95		SF
³⁶² 132	10.11			5.70	4.88	4.29	5.52	3.00	-955.45	0.14		7.61	0.47		SF
³⁶³ 132	10.07			6.90	5.95	4.40	5.63	3.86	-962.58	-0.15		7.07	93.35		SF
³⁶⁴ 132	10.07			5.83	4.98	4.40	5.62	3.11	-1042.94	-0.37		6.73	41.85		SF
³⁶⁵ 132	10.08			6.86	5.89	4.37	5.57	3.83	-1047.26	-0.58		5.66	7.56		SF
³⁶⁶ 132	10.11			5.70	4.81	4.29	5.46	3.00	-1133.40	-0.75		5.78	49.94		SF
³⁶⁷ 132	10.11			6.77	5.76	4.29	5.44	3.75	-1134.74	-0.89		5.01	2.06		SF
³⁶⁸ 132	10.12			5.67	4.75	4.26	5.39	2.97	-1226.78	-1.01		5.30	85.03		SF

Table 6. Table V is continued.

Nuclei	Q_α (cal.) MeV	$\log(T_{1/2}^\alpha)$					$\log(T_{SF})$ Ren-Xu	Q_β (cal.) MeV	Fiset-Nix		Mode of decay
		VSS	GLDM	Brown	Royer	Ni et. al.			$\log(T_{1/2}^\beta)$	$T_{1/2}^\beta$ (sec)	
³⁶⁹ 132	10.13	6.70	5.66	4.23	5.34	3.69	-1224.99	-1.15	4.57	17.96	SF
³⁷⁰ 132	10.09	5.77	4.82	4.34	5.46	3.06	-1323.05	-1.32	4.82	40.63	SF
³⁷¹ 132	10.10	6.80	5.73	4.32	5.41	3.78	-1317.95	-1.51	4.06	42.84	SF
³⁷² 132	10.02	6.00	5.01	4.54	5.66	3.26	-1422.15	-1.66	4.38	43.54	SF
³⁷³ 132	9.60	8.50	7.39	5.75	7.07	5.23	-1413.60	-2.05	3.45	6.48	SF
³⁷⁴ 132	9.29	8.56	7.53	6.69	8.17	5.45	-1524.03	-2.19	3.81	46.12	SF
³⁷⁵ 132	8.96	10.89	9.73	7.75	9.41	7.27	-1511.88	-2.34	3.17	84.63	SF
³⁷⁶ 132	8.75	10.67	9.59	8.46	10.23	7.24	-1628.66	-2.50	3.53	81.95	SF
³⁷⁷ 132	8.80	11.53	10.34	8.29	10.01	7.82	-1612.75	-2.67	2.89	74.83	SF
³⁷⁸ 132	8.67	11.00	9.88	8.73	10.52	7.52	-1735.99	-2.83	3.26	24.58	SF
³⁷⁹ 132	8.54	12.60	11.37	9.19	11.04	8.73	-1716.17	-2.98	2.65	46.56	SF
³⁸⁰ 132	8.43	12.01	10.85	9.58	11.49	8.39	-1845.97	-3.16	3.02	44.02	SF
³⁸¹ 132	8.32	13.55	12.28	9.99	11.95	9.54	-1822.11	-3.33	2.40	53.46	SF
³⁸² 132	8.33	12.44	11.26	9.95	11.90	8.76	-1958.57	-3.57	2.75	56.94	SF
³⁸³ 132	8.43	13.07	11.78	9.58	11.45	9.13	-1930.51	-3.90	2.05	11.26	SF
³⁸⁴ 132	8.50	11.71	10.49	9.33	11.14	8.13	-2073.74	-4.16	2.40	49.43	SF
³⁸⁵ 132	8.61	12.31	10.99	8.94	10.66	8.48	-2041.35	-4.41	1.76	58.11	SF
³⁸⁶ 132	8.49	11.75	10.51	9.37	11.15	8.17	-2191.45	-4.48	2.23	68.76	SF
³⁸⁷ 132	8.78	11.61	10.27	8.36	9.94	7.88	-2154.58	-4.83	1.55	35.80	SF
³⁸⁸ 132	8.69	10.91	9.64	8.67	10.29	7.45	-2311.65	-5.05	1.95	88.81	SF
³⁸⁹ 132	8.62	12.27	10.89	8.91	10.56	8.45	-2270.17	-5.21	1.38	23.86	SF
³⁹⁰ 132	3.00	61.12	59.48	50.81	60.04	50.30	-2434.31	-5.15	1.91	80.36	SF
³⁹¹ 132	2.81	66.23	64.41	54.21	64.04	54.51	-2388.08	-5.83	1.11	12.96	SF
³⁹² 132	2.73	66.99	65.28	55.74	65.84	55.32	-2559.39	-6.07	1.52	32.78	SF

**Fig. 9.** Same as Fig. 7 but for ³⁷⁰132.

3.6.1 Alpha decay

A significant advancement has been made for estimating the alpha decay half-lives since the earliest formulation of Geiger and Nuttall [78]. The calculation of α decay half life $T_{1/2}^\alpha$ requires the Q_α as input. The knowledge of Q_α of a nucleus gives a valuable information about its stability. The estimation of Q_α is done by knowing the binding energies of the parent and daughter nuclei and binding energy

of the ⁴He. The binding energies are calculated using the versatile and powerful framework of relativistic mean-field theory. The Q_α energy is estimated using the relation

$$Q_\alpha(N, Z) = BE(N, Z) - BE(N - 2, Z - 2) - BE(2, 2) \quad (12)$$

Here, $BE(N, Z)$, $BE(N - 2, Z - 2)$, and $BE(2, 2)$ are the binding energies of the parent, daughter and ⁴He ($BE = 28.296$ MeV [79]) with neutron number N and proton number Z . With the even-even values available at hand, the alpha decay half-life of the isotopic chain under study is estimated by Viola-Seaborg semi-empirical relation

$$\log_{10} T_{1/2}^\alpha(sec) = \frac{aZ - b}{\sqrt{Q_\alpha}} - (cZ + d) + h_{\log} \quad (13)$$

The values of the parameters a , b , c and d are taken from the recent modified parametrizations of Sobczewski et al [8], which are $a = 1.66175$, $b = 8.5166$, $c = 0.20$, $d = 33.9069$. The h_{\log} is the hindrance factor which takes into account the hindrance associated with odd proton and neutron numbers as given by Viola and Seaborg

$$h_{\log} = \begin{cases} 0 & \text{even-even;} \\ 0.772 & \text{odd-even;} \\ 1.066 & \text{even-odd;} \\ 1.114 & \text{odd-odd;} \end{cases} \quad (14)$$

The Q_α values obtained from RMF calculations are listed in the Tables 5 - 8. There are also several phenomenological formulas available in the literature for calculating the

Table 7. Same as Table 5 but for $Z = 138$ isotopic chain.

Nuclei	$Q_\alpha(\text{cal.})$	$\log(T_{1/2}^\alpha)$						$\log(T_{SF})$	$Q_\beta(\text{cal.})$	Fiset-Nix		Mode of decay
	MeV	VSS	GLDM	Brown	Royer	Ni et. al.	Ren-Xu		MeV	$\log(T_{1/2}^\beta)$	$T_{1/2}^\beta(\text{sec})$	
³¹⁸ 138	7.62	18.17	18.31	14.50	18.92	13.77	109.15	14.13	-0.68	0.21		β
³¹⁹ 138	7.10	22.11	22.08	16.87	21.75	16.97	98.02	13.83	-1.12	0.08		β
³²⁰ 138	6.52	24.65	24.70	19.84	25.31	19.30	131.77	13.50	-0.56	0.27		β
³²¹ 138	6.05	29.01	28.89	22.56	28.55	22.86	117.23	13.15	-0.99	0.10		β
³²² 138	5.58	31.65	31.60	25.61	32.20	25.27	149.00	12.77	-0.42	0.38		β
³²³ 138	16.86	-6.98	-6.80	-7.09	-7.11	-7.83	131.31	12.37	-0.84	0.15		α
³²⁴ 138	17.10	-8.43	-8.17	-7.40	-7.51	-8.90	160.94	11.90	-0.24	0.58		α
³²⁵ 138	17.06	-7.30	-7.15	-7.35	-7.46	-8.10	140.38	11.82	-0.72	0.19		α
³²⁶ 138	16.93	-8.16	-7.94	-7.18	-7.28	-8.68	167.70	11.57	-0.17	0.68		α
³²⁷ 138	16.64	-6.63	-6.52	-6.79	-6.83	-7.53	144.51	11.35	-0.62	0.24		α
³²⁸ 138	16.50	-7.46	-7.29	-6.61	-6.62	-8.08	169.36	11.17	-0.08	0.84		α
³²⁹ 138	16.29	-6.05	-5.98	-6.32	-6.29	-7.04	143.81	11.02	-0.54	0.29		α
³³⁰ 138	16.12	-6.83	-6.69	-6.08	-6.03	-7.54	166.01	10.75	0.02	1.05		α
³³¹ 138	15.99	-5.54	-5.51	-5.90	-5.82	-6.60	138.35	10.47	-0.41	0.39		α
³³² 138	15.86	-6.38	-6.29	-5.71	-5.62	-7.16	157.75	10.21	0.15	1.43		α
³³³ 138	15.76	-5.14	-5.14	-5.57	-5.46	-6.26	128.23	9.97	-0.28	0.52		α
³³⁴ 138	15.73	-6.15	-6.10	-5.52	-5.43	-6.96	144.67	9.74	0.27	1.88		α
³³⁵ 138	15.63	-4.90	-4.95	-5.38	-5.27	-6.06	113.52	9.51	-0.16	0.69		α
³³⁶ 138	18.11	-9.94	-9.89	-8.64	-9.21	-10.19	126.85	9.83	0.25	1.80		α
³³⁷ 138	15.61	-4.87	-4.95	-5.35	-5.27	-6.03	94.31	9.06	-0.04	0.91		α
³³⁸ 138	15.56	-5.85	-5.87	-5.27	-5.19	-6.70	104.38	8.80	0.53	3.39		α
³³⁹ 138	15.52	-4.71	-4.82	-5.21	-5.14	-5.90	70.68	8.50	0.12	1.32		α
³⁴⁰ 138	15.28	-5.33	-5.40	-4.85	-4.72	-6.27	77.33	8.21	0.70	5.06		α
³⁴¹ 138	15.07	-3.88	-4.03	-4.53	-4.35	-5.19	42.71	7.93	0.29	1.96		α
³⁴² 138	14.82	-4.46	-4.57	-4.14	-3.90	-5.53	45.79	7.63	0.89	7.70		α
³⁴³ 138	14.70	-3.17	-3.36	-3.94	-3.68	-4.58	10.46	7.24	0.52	3.29		α
³⁴⁴ 138	14.63	-4.09	-4.24	-3.83	-3.56	-5.21	9.84	6.95	1.12	13.08		α
³⁴⁵ 138	14.27	-2.30	-2.54	-3.24	-2.86	-3.85	-25.97	6.93	0.63	4.24		SF
³⁴⁶ 138	13.90	-2.60	-2.79	-2.60	-2.11	-3.93	-30.44	6.63	1.23	17.14		SF
³⁴⁷ 138	13.98	-1.70	-1.97	-2.74	-2.30	-3.33	-66.53	6.21	0.90	7.85		SF
³⁴⁸ 138	14.06	-2.94	-3.16	-2.88	-2.48	-4.22	-75.00	5.88	1.53	33.58		SF
³⁴⁹ 138	13.96	-1.66	-1.96	-2.70	-2.29	-3.30	-111.14	5.60	1.15	14.00		SF
³⁵⁰ 138	13.47	-1.66	-1.93	-1.83	-1.25	-3.13	-123.73	5.59	1.65	44.68		SF
³⁵¹ 138	21.29	-12.90	-13.13	-11.96	-13.45	-12.88	-159.73	4.78	1.52	33.45		SF
³⁵² 138	21.00	-13.64	-13.84	-11.69	-13.14	-13.35	-176.59	5.96	1.50	31.60		SF
³⁵³ 138	14.25	-2.26	-2.63	-3.20	-2.95	-3.81	-212.23	5.42	1.23	16.98		SF
³⁵⁴ 138	14.19	-3.21	-3.53	-3.10	-2.85	-4.45	-233.50	5.23	1.81	65.25		SF
³⁵⁵ 138	14.12	-1.99	-2.39	-2.98	-2.72	-3.58	-268.58	5.03	1.41	25.71		SF
³⁵⁶ 138	14.04	-2.89	-3.25	-2.84	-2.57	-4.19	-294.38	4.82	2.01	2.47		SF
³⁵⁷ 138	13.96	-1.66	-2.09	-2.70	-2.42	-3.30	-328.72	4.61	1.62	41.54		SF
³⁵⁸ 138	13.86	-2.51	-2.91	-2.53	-2.23	-3.86	-359.18	4.39	2.23	70.91		SF
³⁵⁹ 138	13.77	-1.25	-1.72	-2.37	-2.05	-2.95	-392.57	4.17	1.86	71.71		SF
³⁶⁰ 138	13.75	-2.27	-2.71	-2.33	-2.03	-3.66	-427.82	3.92	2.50	15.10		SF
³⁶¹ 138	13.68	-1.06	-1.56	-2.21	-1.89	-2.78	-460.08	3.66	2.16	44.27		SF
³⁶² 138	13.45	-1.61	-2.09	-1.79	-1.40	-3.10	-500.25	3.55	2.73	35.38		SF
³⁶³ 138	13.32	-0.26	-0.80	-1.55	-1.13	-2.10	-531.19	3.28	2.41	57.69		SF
³⁶⁴ 138	18.19	-10.05	-10.48	-8.74	-9.79	-10.29	-576.40	3.03	3.09	26.59		SF
³⁶⁵ 138	13.17	0.09	-0.49	-1.27	-0.82	-1.81	-605.83	2.86	2.72	24.89		SF
³⁶⁶ 138	13.05	-0.70	-1.24	-1.04	-0.56	-2.32	-656.21	2.75	3.31	24.64		SF
³⁶⁷ 138	12.96	0.58	-0.03	-0.86	-0.37	-1.39	-683.96	2.62	2.92	23.22		SF
³⁶⁸ 138	12.97	-0.51	-1.09	-0.88	-0.41	-2.16	-739.63	2.44	3.57	12.25		SF
³⁶⁹ 138	13.03	0.41	-0.23	-1.00	-0.56	-1.53	-765.51	2.24	3.26	1.67		SF
³⁷⁰ 138	13.10	-0.82	-1.43	-1.13	-0.74	-2.42	-826.58	1.98	4.01	32.98		SF
³⁷¹ 138	13.30	-0.21	-0.88	-1.51	-1.21	-2.06	-850.43	1.64	3.90	40.22		SF
³⁷² 138	13.52	-1.77	-2.41	-1.92	-1.72	-3.23	-917.02	1.33	4.81	71.40		SF
³⁷³ 138	13.58	-0.84	-1.53	-2.03	-1.86	-2.60	-938.66	1.14	4.59	28.37		SF
³⁷⁴ 138	13.69	-2.14	-2.81	-2.23	-2.12	-3.55	-1010.89	1.01	5.31	30.23		SF

Table 8. Table VII is continued

Nuclei	$Q_\alpha(\text{cal.})$	$\log(T_{1/2}^\alpha)$					$\log(T_{SF})$	$Q_\beta(\text{cal.})$	Fiset-Nix		Mode of decay
	MeV	VSS	GLDM	Brown	Royer	Ni et. al.	Ren-Xu	MeV	$\log(T_{1/2}^\beta)$	$T_{1/2}^\beta(\text{sec})$	
³⁷⁵ 138	10.54	7.26	6.46	4.64	6.12	4.31	-1030.16	1.59	3.97	70.88	SF
³⁷⁶ 138	10.12	7.59	6.81	5.79	7.48	4.75	-1108.13	1.09	5.18	7.04	SF
³⁷⁷ 138	9.92	9.35	8.50	6.36	8.16	6.09	-1124.86	0.76	5.28	26.15	SF
³⁷⁸ 138	12.47	0.71	-0.05	0.12	0.64	-1.12	-1208.70	0.31	6.94	20.87	SF
³⁷⁹ 138	16.40	-6.23	-6.96	-6.47	-7.30	-7.20	-1222.72	0.10	7.37	93.17	SF
³⁸⁰ 138	16.24	-7.03	-7.75	-6.25	-7.05	-7.71	-1312.53	-0.05	8.28	29.55	SF
³⁸¹ 138	16.01	-5.57	-6.34	-5.93	-6.67	-6.63	-1323.69	-0.22	6.78	43.46	SF
³⁸² 138	15.94	-6.52	-7.27	-5.83	-6.57	-7.28	-1419.59	-0.44	6.55	20.71	SF
³⁸³ 138	11.78	3.58	2.69	1.61	2.35	1.17	-1427.72	-0.48	5.95	93.97	SF
³⁸⁴ 138	11.53	3.21	2.33	2.18	3.02	1.01	-1529.80	-0.33	6.89	97.30	SF
³⁸⁵ 138	11.43	4.56	3.63	2.41	3.29	2.00	-1534.76	-0.49	5.92	52.09	SF
³⁸⁶ 138	11.28	3.92	3.01	2.77	3.70	1.62	-1643.14	-0.65	6.03	31.62	SF
³⁸⁷ 138	11.21	5.19	4.23	2.94	3.89	2.55	-1644.77	-0.78	5.26	66.55	SF
³⁸⁸ 138	11.12	4.39	3.45	3.16	4.14	2.03	-1759.55	-0.90	5.52	88.02	SF
³⁸⁹ 138	11.09	5.55	4.56	3.23	4.21	2.85	-1757.70	-1.00	4.85	7.15	SF
³⁹⁰ 138	11.01	4.72	3.74	3.43	4.43	2.31	-1878.98	-1.10	5.18	45.38	SF
³⁹¹ 138	10.81	6.40	5.37	3.93	5.02	3.58	-1873.50	-1.18	4.56	59.33	SF
³⁹² 138	10.65	5.84	4.82	4.35	5.51	3.26	-2001.38	-1.26	4.94	61.70	SF
³⁹³ 138	10.43	7.61	6.54	4.93	6.19	4.61	-1992.14	-1.35	4.31	29.21	SF
³⁹⁴ 138	10.27	7.08	6.02	5.37	6.70	4.32	-2126.72	-1.46	4.66	49.79	SF
³⁹⁵ 138	3.82	52.22	50.69	41.66	50.31	42.64	-2113.56	-4.78	1.59	38.93	SF
³⁹⁶ 138	3.70	52.97	51.48	43.16	52.10	43.44	-2254.94	-3.08	3.10	59.17	SF
³⁹⁷ 138	3.68	54.35	52.77	43.42	52.39	44.46	-2237.73	-3.31	2.44	76.36	SF
³⁹⁸ 138	9.52	9.74	8.59	7.56	9.28	6.59	-2386.00	-3.47	2.83	82.99	SF

alpha decay half-lives. The semi-empirical formula proposed by Brown [73] for determining the half-life of superheavy nuclei is given by

$$\log_{10} T_{1/2}^\alpha(\text{sec}) = 9.54(Z-2)^{0.6}/\sqrt{Q_\alpha} - 51.37 \quad (15)$$

where Z is the atomic number of parent nucleus and Q_α is in MeV. Another formula proposed by Dasgupta-Schubert and Reyes [72] based on generalized liquid drop model and obtained by fitting the experimental half-lives for 373 alpha emitters for determining the half-lives of superheavy nuclei is given as

$$\log_{10} T_{1/2}^\alpha(\text{sec}) = a + bA^{1/6}Z^{1/2} + cZ/Q_\alpha^{1/2} \quad (16)$$

The parameters a, b and c are given by

$$a, b, c = \begin{cases} -25.31, -1.1629, 1.5864 & \text{even-even}; \\ -26.65, -1.0859, 1.5848 & \text{even-odd}; \\ -25.68, -1.1423, 1.5920 & \text{even-odd}; \\ -29.48, -1.113, 1.6971 & \text{odd-odd}; \end{cases} \quad (17)$$

In Ref. [75] Ni et. al. proposed a unified formula for determining the half-lives in alpha decay and cluster radioactivity. The formula for alpha decay is written as

$$\log_{10} T_{1/2}^\alpha(\text{sec}) = 2a\sqrt{\mu}(Z-2)Q_\alpha^{-1/2} + b\sqrt{\mu}[2(Z-2)]^{-1/2} + c \quad (18)$$

Where, a, b, c are the constants and μ is define as $4(A-4)/A$. Recently, Royer estimated the potential energy during α emission within liquid drop model including the

proximity effects between α particle and the daughter nucleus and the α decay half-lives were calculated from the WKB barrier penetration probability analogous to asymmetric spontaneous fission. The theoretical predictions for half-life for heavy and superheavy nuclei by employing a fitting procedure to a set of 373 alpha emitters was developed by Royer [74] with an RMS derivation of 0.42, given as

$$\log_{10} T_{1/2}(\text{sec}) = -26.06 - 1.114A^{1/6}\sqrt{Z} + \frac{1.5837Z}{\sqrt{Q_\alpha}} \quad (19)$$

where A and Z represent respectively the mass number and charge number of the parent nuclei and Q_α represents the energy released during the reaction. Assuming a similar dependence on A, Z and Q_α , the above equation was reformulated for a subset of 131 even-even nuclei and a relation was obtained with a RMS derivation of only 0.285, given, as

$$\log_{10} T_{1/2}^\alpha(\text{sec}) = -25.31 - 1.1629A^{1/6}\sqrt{Z} + \frac{1.5864Z}{\sqrt{Q_\alpha}} \quad (20)$$

For a subset of 106 even-odd nuclei, the relation given by was further modified with an RMS derivation of 0.39, and is given as,

$$\log_{10} T_{1/2}^\alpha(\text{sec}) = -26.65 - 1.0859A^{1/6}\sqrt{Z} + \frac{1.5848Z}{\sqrt{Q_\alpha}} \quad (21)$$

A similar reformulation was performed for the equation for a subset of 86 odd-even nuclei and 50 odd-odd nuclei.

3.6.2 Beta decay

Beta decay is also a very important decay mode for proton-rich and neutron-rich nuclei. Fermi theory of β decay involves electron-neutrino interaction, which describes the beta transition rates according to $\log(ft)$ values. We employed the empirical formula of Fiset and Nix [77] for estimating the half-lives of the isotopic chain under study and is given as

$$T_\beta = 540 \times 10^{5.0} \frac{m_e^5}{\rho_{d.o.s.}(W_\beta^6 - m_e^6)} \quad (22)$$

In an analogous way to α decay, we evaluate the Q_β value using the relation $Q_\beta = BE(Z+1, A) - B(Z, A)$ and $W_\beta = Q_\beta + m_e$. Here, $\rho_{d.o.s.}$ is the average density of states in the daughter nucleus ($e^{-A/290} \times$ number of states within 1 MeV of ground state).

3.6.3 Spontaneous Fission

The determination of spontaneous half-lives helps in identifying the long lived superheavy elements and mode of decay of heavy and superheavy nuclei. Several empirical formulas have been proposed by various authors from time to time for determining the spontaneous fission half-lives. In our calculations, we employed the phenomenological formula proposed by Ren and Xu [76] and is given by

$$\begin{aligned} \log_{10} T_{1/2}^\alpha(\text{sec}) = & 21.08 + C_1 \frac{(Z-90-\nu)}{A} + C_2 \frac{(Z-90-\nu)^2}{A} \\ & + C_3 \frac{(Z-90-\nu)^3}{A} \\ & + C_4 \frac{(Z-90-\nu)(N-Z-52)^2}{A} \end{aligned} \quad (23)$$

Where, Z , N , A represent the proton, neutron and mass number of parent nuclei. C_1 , C_2 , C_3 , C_4 are the empirical constants and ν is the seniority term which takes care of blocking effect of unpaired nucleons on the transfer of many nucleon pairs during the fission process.

Our study on modes of decay highlights the range of isotopes which survive fission and thus decay through alpha emission. Alpha and beta decay energies, Q_α , Q_β estimated by RMF binding energy is in quite agreement with FRDM data as given in Table 5. However, calculated half-lives by RMF do not match well with FRDM values. This is why because $T_\alpha \propto 10^{\frac{1}{\sqrt{Q_\alpha}}}$ and $T_\beta \propto \frac{1}{Q_\beta^5}$ indicates that a small change in Q_α and Q_β creates a big difference in T_α and T_β as reflected in Tables 5 - 8. The calculated alpha decay half-lives using VSS, GLDM, Brown, Royer and NI et al. are tabulated in Tables 5 - 8 and a good agreement among them as well as with macro-microscopic data is noticed. To check the possibility of β -decay empirical Fiset and Nix formula is employed to calculate the β -decay half-life for the considered isotopic chain and the results are given in Tables 5 - 8. The beta decay half-lives are found to be very large than alpha decay as well as spontaneous fission half-lives and hence there is no possibility of mode

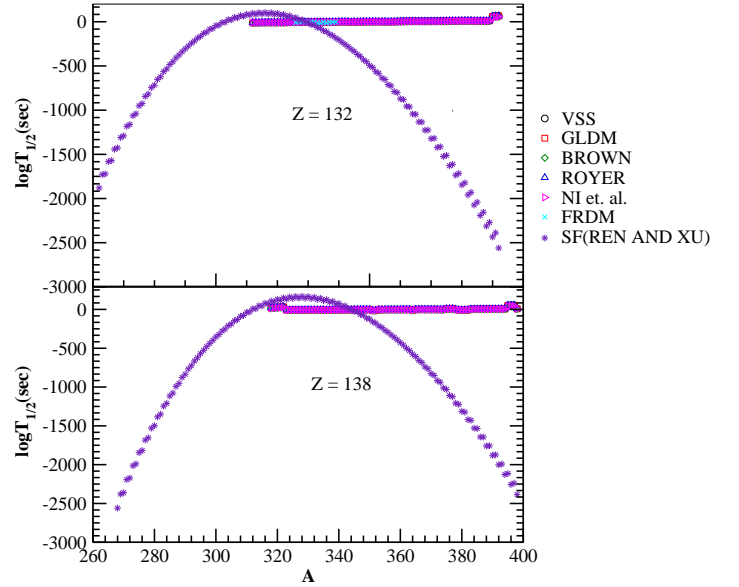


Fig. 10. (color online) Alpha decay and spontaneous fission half-lives of $Z = 132, 138$ isotopic chain as a function of mass number.

of beta decay in present considered isotopes. Further, SF half-lives is calculated and the values are framed in one of the columns of Tables 5 - 8. Also, the alpha decay and SF half-lives for considered isotopic chain are plotted in Figure 10. After analyzing the concerned Tables and Figure, the analysis predicts that the isotopes of $Z = 132$ with a mass range $312 \leq A \leq 329$ survive the fission and may be observed through alpha decay and those nuclei beyond $A > 329$ do not survive the fission and hence completely undergo spontaneous fission. For $Z = 138$, the nuclides with a mass range $323 \leq A \leq 344$ survive the fission and are observed through alpha decay in the laboratory while the nuclei beyond $A > 344$ do not survive fission and end with spontaneous fission. In the first five isotopes $^{318-322}138$, beta decay is the dominant mode of decay. Therefore, the present study reveals that alpha decay and spontaneous fission are the principal modes of decay of majority of the considered nuclides with beta decay as the principal mode of decay in the first five isotopes of $Z = 138$.

4 Summary

We calculated the structural properties of $Z = 132, 138$ superheavy nuclei with a range of neutron $N = 180 - 260$ within axially deformed relativistic mean field theory. The calculations are performed for prolate, oblate and spherical configurations in which prolate is suggested to be the ground state. The results produced by RMF are in good agreement with FRDM data. Density distribution has been made to explain the special features of the nuclei such as bubble structure or halo structure. Bubble structure is seen for some of the cases of the nuclei. To make the clear presentation of nucleon distribution for some of the selected nuclei, the two-dimensional contour

plot of density has been made by which cluster and bubble type structure is revealed. Further, the predictions of possible modes of decay such as alpha decay, beta decay and spontaneous fission of the isotopes of $Z = 132$ and $Z = 138$ in the neutron range $180 \leq N \leq 260$ have been done within self-consistent model. The calculation of half-lives computed using Viola-Seaborg, GLDM, Brown, Royer and Ni et. al., show good agreement with each other as well as with macro-microscopic FRDM data. All the physical observables calculated by RMF are found in good agreement with FRDM data. Also, the extensive study on beta decay half-lives and SF half-lives of the considered isotopic chain under investigations been made to identify the mode of the decay of these isotopes. The study reveals that the isotopes of $Z = 132$ that fall within the mass range $312 \leq A \leq 329$ undergoes alpha decay and those with mass number $A > 329$ do not survive fission and hence completely undergoes spontaneous fission. For $Z = 138$, the alpha decay occurs within the isotopic mass chain $318 \leq A \leq 344$ and the isotopes beyond $A > 344$ the mass range do not survive fission and end up with spontaneous fission. The present analysis reveals that α -decay and SF are the principal modes of decay in majority of the isotopes of superheavy nuclei under study in addition to β decay being the principal mode of decay in $^{318-322}_{138}$ isotopes. Hence, we hope that present theoretical predictions on possible decay modes of $Z = 132, 138$ superheavy nuclei might pave the way to help and guide the experimentalists in future for the synthesis of new superheavy isotopes.

5 Acknowledgments

One of the authors (MI) would like to acknowledge the hospitality provided by Institute of Physics (IOP), Bhubaneswar during the work.

References

1. W. D. Myers, W. J. Swiatecki, Nucl. Phys. A **81**, 1 (1966).
2. A. Sobiczewski, F. A. Gareev, B. N. Kalinkin, Phys. Lett. **22**, 500 (1966).
3. H. Meldner, Ark. Fys. **36**, 593 (1967).
4. S. G. Nilsson, C. F. Tsang, A. Sobiczewski, Z. Szymanski, S. Wycech, C. Gustafson, I. L. Lamm, P. Möller, B. Nilsson, Nucl. Phys. A **131**, 1 (1969).
5. U. Mosel, W. Greiner, Z. Phys. **222**, 261 (1969).
6. P. Möller, J. R. Nix, W. D. Wyers, and W. J. Swiatecki, At. Data Nucl. Data Tables **59**, (1999) 185; P. Möller, J. R. Nix and K. L. Kratz *ibid.*, **66**, 131 (1997).
7. S. C. Cwiok, V. V. Pashkevich, J. Dudek, W. Nazarewicz, Nucl. Phys. A **41**, 254 (1983).
8. A. Sobiczewski, Z. Patyk, S. C. Cwiok, Phys. Lett. B **224**, 1 (1989).
9. Z. Patyk, A. Sobiczewski, Nucl. Phys. A **533**, 132 (1991).
10. D. N. Poenaru, M. Ivascu, A. Sandulescu, and W. Greiner, Phys. Rev. C **32**, 572 (1985).
11. B. Buck, A. C. Merchant, and S. M. Perez, Phys. Rev. C **45**, 2247 (1992).
12. D. N. Basu, Phys. Lett. B **566**, 90 (2003).
13. H. F. Zhang and G. Royer, Phys. Rev. C **76**, 047304 (2007).
14. M. M. Sharma, A. R. Farhan, and G. Munzenberg, Phys. Rev. C **71**, 054310 (2005).
15. J. C. Pei, F. R. Xu, Z. J. Lin, and E. G. Zhao, Phys. Rev. C **76** 044326(2007).
16. S. Hoffman, G. Munzenberg, Rev. Mod. Phys. **72**, 733 (2000).
17. S. Hoffman et. al., Z. Phys. A **350**, 277 (1995).
18. S. Hoffman et. al **358**, 125 (1997).
19. S. Hoffman et. al., Z. Phys. A **350**, 281 (1995).
20. S. Hoffman et.al., Z. Phys. A **354**, 229 (1996).
21. S. Hoffman, G. Munzenberg, Rev. Mod. Phys. **72**, 733 (2000).
22. K. Morita et. al., J. Phys. Soc. Japan **73**, 2593 (2004).
23. K. Morita et. al., Nucl. Phys. A **734**, 101 (2004).
24. Yu. Ts Oganessian et. al., Phys. Rev. Lett 109.162501 (2012).
25. Yu. Ts Oganessian et. al., Phys. At. Nucl. 64 1349 (2001).
26. Yu. Ts Oganessian et. al., Phys. Rev. C 72, 034611 (2005).
27. Yu. Ts Oganessian et. al., Phys. At. Nucl. 63, 1679 (2000).
28. Yu. Ts. Oganessian, J. Phys. G: Nucl. Part. Phys. **34**, R165 (2007).
29. J. Dvorak et. al., Phys. Rev. Lett. **97**, 242501 (2006).
30. Yu. Ts. Oganessian et. al., Phys. Rev. C **79**, 024603 (2009).
31. D. N. Poenaru et. al., At. Data Nucl. Data Tables **34**, 423 (1986).
32. D. N. Poenaru, I. H. Plonski, and W. Greiner, Phys. Rev. C **74**, 014312 (2006).
33. D. N. Poenaru, I. H. Plonski, R. A. Ghergesu, and W. Greiner, J. Phys. G: Nucl. part. Phys. **32**, 1223 (2006).
34. C. Samanta, D. N. Basu, and P. R. Chowdhary, J. Phys. Soc. Japan **76** 124201 (2007).
35. D. S. Delin, R. J. Liotta and R. Wyss, Phys. Rev. C **76**, 044301(2007).
36. H. J. Rose and G. A. Jones, Nature **307**, 245 (1984).
37. E. Hourani, M. Hussonnois and D. N. Poenaru, Annales de Physique **14**, 311(1989).
38. A. Sandulescu, D. N. Poenaru and W. Greiner, Sovt. Jour. Nucl. Phys. **11**, 528 (1980).
39. B. K. Sharma, P. Arumugam, S. K. Patra, P. D. Stevenson, R. K. Gupta and W. Greiner, J. Phys. G **32**, L1 (2006).
40. C. Qi, F. R. Xu, R. J. Liotta and R. Wyss, Phys. Rev. Lett **103**, (2009).
41. D. N. Poenaru, R. A. Gherghescu and W. Greiner Phys. Rev. C **83**, 014601 (2011).
42. D. N. Poenaru, R. A. Gherghescu and W. Greiner Phys. Rev. Lett. **107**, 062503 (2011).
43. D. N. Poenaru, R. A. Gherghescu and W. Greiner, J. Phys. G **39**, 015105 (2012).
44. D. N. Poenaru, R. A. Gherghescu and W. Greiner Phys. Rev. C **85**, 034615 (2012).
45. A. V. Karpov and V. I. Zagrebaev, Int. J. Mod. Phys. E **21**, 1250013 (2012).
46. N. Bohr and J. A. Wheeler, Phys.Rev. **56**, 426 (1939).
47. G. N. Flerov and K. A. Petrjak, Phys. Rev. **58**, 89 (1940).
48. W. J. Swiatecki, Phys. Rev. **100**, 937 (1955).
49. Z. Ren and C. Xu, Nucl. Phys. A **759**, 64 (2005).
50. C. Xu and Z. Ren, Phys. Rev. C **71**, 014309 (2005).
51. C. Xu, Z. Ren and Y. Guo, Phys. Rev. C **78**, 044329 (2008).
52. B. D. Serot, Rep. Prog. Phys. **55**, 1855 (1992).
53. Y. K. Gambhir, P. Ring, and A. Thimet, Ann. Phys. (N.Y.) **198**, 132(1990).

54. P. Ring, Prog. Part. Nucl. Phys. **37**, 193 (1996).
55. B. D. Serot and J. D. Walecka, Adv. Nucl. **16**, 1 (1986).
56. J. Boguta, and A. R. Bodmer, Nucl. Phys. A **292**, 413 (1977).
57. T. Sil, S. K. Patra, B. K. Sharma, M. Centelles and X. Viñas, Phys. Rev. C **69**, 044315 (2004).
58. D. G. Madland, R. J. Nix, Nucl. Phys. A **476**, 1 (1988).
59. G. A. Lalazissis, S. Karatzikos, R. Fossion, D. Pena Arteaga, A. V. Afanasjev, and P. Ring, Phys. Lett. **671**, 36 (2009).
60. W. Zhang, J. Meng, S. Q. Zhang, L. S. Gang and H. Toki, Nucl. Phys. A **753**, 106 (2005).
61. M. Bhuyan and S. K. Patra, Mod. Phys. Lett. A **27**, 1250173 (2012).
62. S. K. Patra and C. R. Praharaj, Phys. Rev. C **47**, 2978 (1993).
63. F. Sarazin et. al., Phys. Rev. Lett. **84**, 5062 (2000).
64. J. L. Egido, L. M. Robeldo, R. R. Rodriguez-Guzman, Phys. Rev. Lett. **93**, 282502 (2004).
65. J. A. Wheeler (unpublished).
66. H. A. Wilson, Phys. Rev. C **69**, 538 (1946).
67. J. Decharge et. al., Nucl. Phys. A **716**, 55 (2003).
68. M. Grasso et. al., Phys. Rev. C **79**, 034318 (2009).
69. S. K. Singh, M. Ikram and S. K. Patra, Int. J. Mod. Phys. E **22**, 1350001 (2013).
70. B. K. Sharma, P. Arumugam, S. K. Patra, P. D. Stevenson, R. K. Gupta and W. Greiner, J. Phys. G: Nucl. Part. Phys. **32**, L1 (2006).
71. V. E. Viola, Jr. and G. T. Seaborg, J. Inorg. Nucl. Chem. **28**, 741 (1966).
72. N. Dasgupta-Schubert and M. A. Reyes, At. Data Nucl. Data Tables **93**, 90 (2007).
73. B. A. Brown, Phys. Rev. C **46**, 811 (1992).
74. G. Royer, J. Phys. G, Nucl. Part. Phys. **26**, 1149 (2000).
75. D. D. Ni , Z. Z. Dong, and T. K et al. Phys. Rev. C, **78**, 044310 (2008).
76. Z. Ren and C. Xu, Nucl. Phys. A **759**, 64 (2005).
77. E. O. Fiset and J. R. Nix, Nucl. Phys. A **193**, 647 (1972).
78. H. Geiger and J. M. Nuttall, Philos. Mag. **22**, 613 (1911); H. Geiger, Z. Phys. **8**, 45 (1922).
79. G. Audi, A. H. Wapstra and C. Thibault, Nucl. Phys. A **729**, 337 (2003).